Concrete Beton, Volume 118, pp 8-14, July 2008

# Shear Failure of Steel Fibre-Reinforce Concrete-based Push Off Tests

Authors: Bryan Barragán[1], Ravindra Gettu[2], Luis Agulló[3] and Raúl Zerbino[4]

[1]Department of Construction Engineering, Universitat Politècnica de Catalunya (UPC), Barcelona, Spain
[2]Indian Institute of Technology, Madras, Chennai, India
[3]Department of Construction Engineering, Universitat Politècnica de Catalunya (UPC), Barcelona, Spain
[4]Department of Construction Engineering, Universidad Nacional de la Plata, La Plata, Argentina

ABSTRACT: This paper presents the results of an experimental study that analyses the shear behaviour of steel fibre-reinforced concrete. Direct shear push-off tests are carried out on normal- and high-strength steel fibre-reinforced specimens. The test can be performed in a stable manner for steel-reinforced concrete, permitting the determination of pre- and post-peak responses, and consequently, characterizing the shear stress that can be transferred across an open crack. The shear stress-slip response is analysed and toughness-based parameters, for possible use in design, are calculated.



Journal Contact Details:
PO Box 75364
Lynnwood Ridge
Pretoria, 0040
South Africa
+27 12 348 5305

CONCRETE SOCIETY
OF SOUTHERN AFRICA

admin@concretesociety.co.za
www.concretesociety.co.za

# Shear failure of steel fibre-reinforced concrete based on push off tests

*by Bryan Barragán, Ravindra Gettu, Luis Agulló, and Raúl Zerbino*

*ACI member* ***Bryan Barragán*** *is a Senior Researcher in the Department of Construction Engineering, Universitat Politècnica de Catalunya (UPC), Barcelona, Spain, where he received his PhD in 2002. His research interests include fibre-reinforced concrete, self consolidating concrete, and mixture design.*

*ACI member* ***Ravindra Gettu*** *is a Professor of Civil Engineering at the Indian Institute of Technology Madras, Chennai, India. His research interests include concrete technology, fibre-reinforced concrete, admixtures, fracture mechanics, and self-consolidating concrete.*

***Luis Agulló*** *is a Professor and Head of the Department of Construction Engineering at UPC. His research interests include concrete technology, behavior of concrete dams, and shotcrete.*

***Raúl Zerbino*** *is an Associate Professor in the Department of Construction Engineering, Universidad Nacional de La Plata, La Plata, Argentina, and CONICET Researcher at LEMIT-CIC, La Plata. His research interests include concrete technology, fibre reinforced concrete, fracture mechanics, and self-consolidating concrete.*

*The paper presents results of an experimental study that analyzes the shear behaviour of steel fibre-reinforced concrete. Direct shear push-off tests are carried out on normal- and high-strength steel fibre-reinforced concrete specimens. The test can be performed in a stable manner for steel fibre-reinforced concrete, permitting the determination of the pre- and post-peak responses and, consequently, characterizing the shear stress that can be transferred across an open crack. The shear stress-slip response is analyzed and toughness-based parameters, for possible use in design, are calculated.*

## Introduction

One of the most promising structural applications of steel fibre-reinforced concrete (SFRC) is the use of fibres as shear reinforcement, due to the brittle nature of shear failure. This is of further importance when dealing with high-strength concrete (HSC), which is inherently more brittle than conventional concrete. Along these lines, some applications of SFRC have been studied[1] for example, to replace stirrups in thin-webbed beams and enhance the web-flange shear transfer in girders. Also, it has been shown that the shear strength and deformability of shear keys in segmental construction, for example, of pre-stressed bridge girders and tunnel linings, can be significantly increased through the use of fibre reinforcement.

The objective of the present study is to characterize the failure and toughness of SFRC subjected to direct shear loading at the material level. With this aim, the push-off test on a double-notched prism is used to quantify the shear stress-displacement behaviour of SFRC. The experimentally obtained shear stress-slip response is used to calculate toughness-based parameters, which can be employed in structural design. Reference tests were also carried out on plain concrete specimens.

## Research significance

The fundamental knowledge of the shear failure and toughness of steel fibre-reinforced concrete is essential for the introduction of ductility or toughness parameters in relevant structural design. If such parameters can be obtained from simple tests, they could be probably used in designs including shear keys, web-flange stress transfer, and punching resistance. Additionally, the validation of a simple test method will facilitate the comparison of the behaviour of different types of SFRC within materials engineering processes aimed at enhancing shear transfer in applications such as slabs and tunnel linings.

## Specimen geometry and test setup

There has been significant interest in determining the response of SFRC under direct shear failure, and several types of specimens have been used for this purpose[2,3].

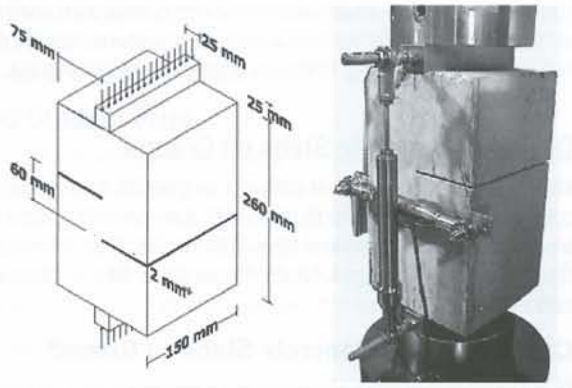


*Fig. 1—Push-off specimen in study.*

The general objective of performing these tests has been to produce shear failure along a prescribed plane (normally defined by cutting notches in the specimen), employing compression and bending loads. One exception is the Japanese JSCE-SF Standard[4], where a double-shear test is performed on un-notched prisms. However, it appears that even in this case, specimens with notches and a single shear plane lead to more representative results[5]. Among the different approaches used, the most popular seems to be the push-off specimen (Fig. 1), made up of two L-shaped blocks that are connected through a ligament along which the shear loading is applied. Previous researchers[2,6-12] have used different types of push-off tests with variations in the specimen dimensions. In some cases, the notches are cast (that is, not cut), which could cause a non-uniform fibre distribution near the notches due to wall effects. To avoid cracking outside the shear plane, some researchers have resorted to using side grooves (which may result in a two-dimensional crack front) and placing reinforcing bars in the blocks (which may interfere with the fibre distribution). The control of the test could also be a problem[13] if an appropriate testing machine is not used.

Taking advantage of the previous experience with this type of test and extending it further, a test geometry and configuration that would permit failure dominated by shear along the vertical plane, at least in the SFRC specimens, were adopted. It was also intended to have a specimen that is based on standard dimensions and easy to handle and test. After several preliminary tests considering different variations of the width of the loading bar, boundary conditions, mode of control, and loading rate, the specimen and test setup given in Fig. 1 were chosen.

The push-off specimen is obtained from one of the halves of a notched or un-notched beam previously tested in flexure after cutting away the part that could be affected by the fracture process.

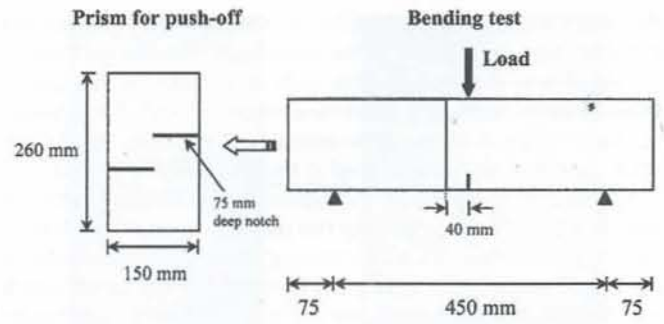


*Fig. 2–Preparation of push-off test specimen.*

This facilitates the use of standard moulds and the same specimen for both flexural and shear tests. In the present study, all the specimens were cut from 150 x 150 x 600 mm notched beams that had been tested under centre point loading, as in Fig. 2. The specimen length was chosen to be 260 mm and two notches of 75 mm length were cut 60 mm apart, perpendicular to the axis of the specimen, as in Fig. 1. The load is applied through steel bars of 25 mm width, and 2 mm thick Teflon sheets are placed between the fixed loading platens of the machine and the bars to compensate for nonparallel loading surfaces.

In discussing such shear tests, one conceptual aspect that has to be addressed is the failure mechanism, which appears to be governed by splitting-tension rather than by shear.

Nevertheless, the tensile stresses are approximately an order of magnitude smaller than the shear stresses and, consequently, shear cracking is expected to dominate the failure when tensile cracking is restrained by the fibres. Moreover, in the present specimen, the use of a ligament length of 60 mm, which is small compared with the total specimen length, helps the development of shear cracking.

To ensure the presence of dominant shear stresses in the ligament, the specimen geometry was studied using elastic finite element analysis (by means of the DRAC code).

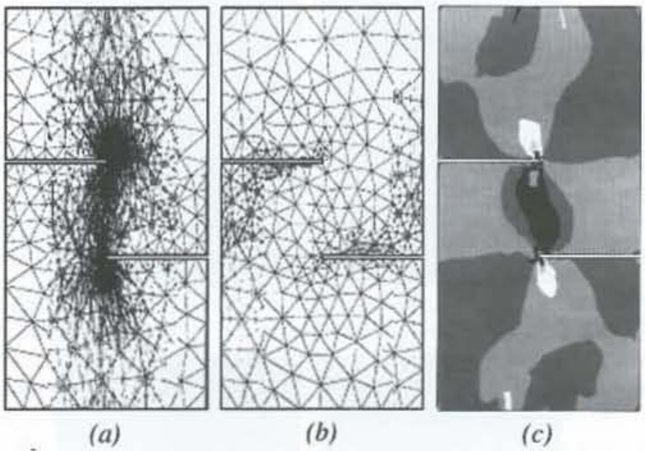


*Fig. 3–Finite element mesh used and distributions of: (a) compressive; (b) tensile; and (c) shear stresses (darker areas indicate higher magnitudes of stress).*

The stress distributions obtained are given in Fig. 3, where it can be seen that high compressive stresses occur along the central plane (Fig. 3(a)) with some tensile stresses near the notch faces (Fig. 3(b)), indicating the possibility of cracking.

The shear stress distribution is shown in Fig. 3(c), with darker zones indicating higher stresses; it can be seen that there is a zone of high shear stresses between the tips of the notches, confirming that shear failure would occur if tensile cracking was to be restrained by the fibres. This was also seen in independent analyses of the same specimens performed at the Politecnico di Milano[14].

The tests were performed in a servo-hydraulic testing system under closed-loop control with a constant piston displacement rate of 0.001 mm/s, which resulted in the peak load occurring at about 5 minutes and a test duration of approximately 30 minutes. Three specimens were tested for each concrete. In addition to the load, displacements were measured by means of linear variable differential transformers (LVDTs) of 2 mm span, mounted horizontally and vertically on one of the faces of the specimen, as in Fig. 1. The vertical LVDT gives the load-line displacement, which is taken as the slip, once the crack has formed. The horizontal LVDT gives the dilatation of the crack or the crack width during the shear failure. All measurements were recorded continuously using the controller and software.

## Materials and specimen preparation

Two concrete mixtures were studied: a normal-strength, 30 MPa concrete, C30, and a high-strength, 70 MPa concrete, C70. Table 1 gives the proportions of the two mixtures. In each mixture, two dosages of steel fibres, 20 and 40 kg/m$^3$, have been incorporated. In both cases, the fibres were non-coated, collated, and hooked-ended, with circular cross sections. The characteristics of the fibres can be seen in Table 2; the fibres denoted as RC-80/60 BN were incorporated in the C30 concrete and the higher-strength fibres, denoted as RC-80/30 BP, were used in C70 concrete. The shorter fibres with higher strength were used in the C70 concrete because such fibres are recommended for high-strength concrete to obtain adequate toughening[15]. Note that direct comparisons cannot be made between the two concretes because the fibre densities are significantly different. The concretes are denoted hereafter by the base concrete denomination followed by the fibre dosage, as in Table 1.

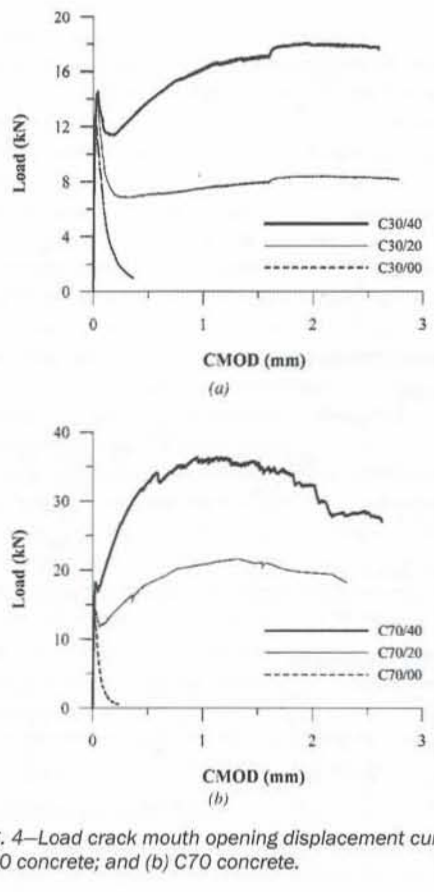


*Fig. 4–Load crack mouth opening displacement curves in flexure for: (a) C30 concrete; and (b) C70 concrete.*

All mixtures were prepared using a 0.25 $m^3$ vertical-axis forced-action mixer. The mixing procedure was as follows.

First, the gravel, sand, cement, and silica fume (in the case of high-strength concrete) were dry-mixed for 1 minute.
Second, water was added and the mixing continued for another minute, after which the high-range water-reducing admixture was incorporated. Lastly, in the case of plain concrete, the mixing was continued for another 3 minutes and then stopped. For the SFRCs, the mixing continued for 2 minutes and then the fibres were incorporated and the components were mixed for another 3 minutes. The mixtures were observed to be homogeneous with adequate workability.

Slump test results of the fresh concretes are presented in Table 3, along with other standard properties. A systematic reduction in the slump with an increase in fibre dosage is observed, as expected. The compressive strength *fc* and modulus of elasticity *E* were obtained through uniaxial compression tests of 150 x 300 mm cylinders at the age of 28 days. No significant influence of the fibres on *fc* and *E* could be identified, though the latter was seen to increase slightly with fibre dosage.

For each concrete, 150 x 150 x 600 mm beams were cast, all from the same batch, and compacted using a 50 Hz vibrating table. The filling of the moulds followed the recommendations of RILEM TC 162-TDF.[16] A preferential orientation of the fibres along horizontal planes can be expected in such specimens[17]. Therefore, it is important that the notch planes have the same orientation, with respect to the casting direction, in all the specimens. The top surfaces of the specimens were finished manually and covered with a plastic sheet. After 24 hours, the specimens were demoulded and placed in a fog room (at 20 °C and 98% relative humidity [RH]) for 28 days, after which they were transferred to the laboratory for testing.

As mentioned previously, the beams were subjected to flexure prior to obtaining the prisms for the push-off tests. In the flexural tests, the specimen with a 25 mm-long notch at midspan (refer to Fig. 2) was tested under three-point bending. The typical load-crack opening (CMOD) curves are shown in Fig. 4. As it can be seen, toughness increases noticeably with fibre dosage and concrete strength, with a tendency toward hardening-type response in the high strength concrete (Fig. 4(b)).

### Table 1—Mixture proportions of concrete

| Components | C30 | | | C70 | | |
|---|---|---|---|---|---|---|
| | C30/00 | C30/20 | C30/40 | C70/00 | C70/20 | C70/40 |
| Cement type CEM 1 52.5 R, kg/$m^3$ | 349 | | | 480 | | |
| 5 to 12 mm gravel, kg/$m^3$ | 978 | | | 921 | | |
| 0 to 5 mm sand, kg/$m^3$ | 873 | | | 840 | | |
| Densified silica fume, kg/$m^3$ | – | | | 48 | | |
| Water added, kg/$m^3$ | 205 | | | 161 | | |
| *w/c* | 0.57 | | | 0.35 | | |
| Naphthalene-based high-range water reducing admixture (solids % by weight of cement) | 0.25 | | | 2 | | |
| RC-80/60 BN fibres, kg/$m^3$ | – | 20 | 40 | – | – | – |
| RC-80/30 BP fibres, kg/$m^3$ | – | – | – | – | 20 | 40 |

### Table 2—Characteristics of fibres used (as provided by supplier)

| Properties | Fibre | |
|---|---|---|
| | RC-80/60 BN | RC-80/30 BP |
| Carbon content | Low | High |
| Length, mm | 60 | 30 |
| Diameter, mm | 0.75 | 0.38 |
| Minimum tensile strenght, Mpa | 1100 | 2300 |
| Modulus of elasticity, GPa | 200 | 200 |

### Table 3—Characteristics of concrete

| Concrete | Slump, mm | $f_c$, MPa | E, GPa | $\pi_u$, MPa |
|---|---|---|---|---|
| 30/00 | 150 | 40.2 | 30.0 | 4.1 |
| 30/20 | 140 | 38.9 | 31.8 | 6.2 |
| 30/40 | 110 | 38.3 | 31.8 | 5.9 |
| 70/00 | 200 | 77.7 | 36.6 | 5.5 |
| 70/20 | 130 | 76.5 | 37.2 | 8.2 |
| 70/40 | 50 | 77.8 | 38.9 | 10.0 |

## Results of push-off tests

### Failure modes

The typical mode of failure in unreinforced (plain) C30 and C70 concretes can be seen, respectively, in Fig. 5 and 6, where the two sides of the same specimen are shown. The first crack initiates on one of the notch faces, at approximately 20 mm from the notch-tip (marked as Point 1 in Fig. 5), and propagates towards the tip of the other notch (that is, Point 2). At about the same time, Crack 2-2 appears (refer to Fig. 5), which could be defined as a shear crack. Sometimes, only one crack of the 1-2 type appears, followed by almost instantaneous splitting failure. Because the cracking is dominated by tensile splitting, this type of test method has been criticized in the literature[18] as being inapplicable for obtaining the shear behaviour of plain concrete.

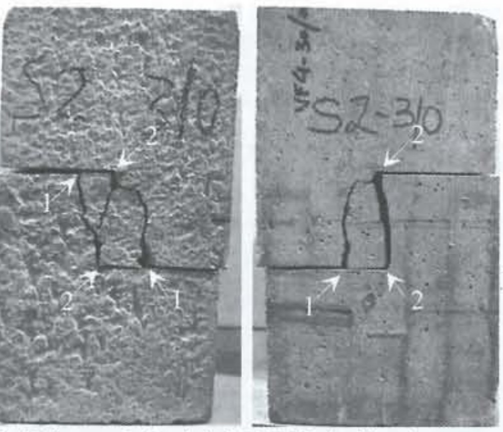


*Fig. 5—Typical failure mode for plain C30/00 (both sides of same specimen).*

*Fig. 6—Typical failure mode for plain C70/00 (both sides of same specimen).*

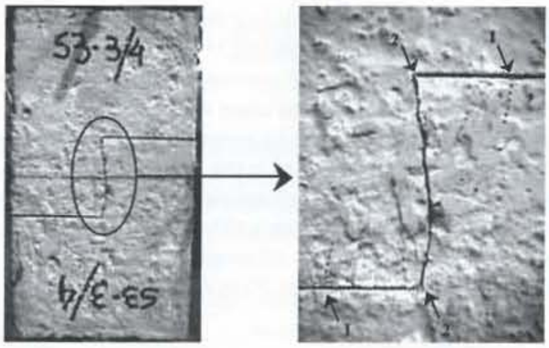

Fig. 7—Typical failure mode for C30/40 (same specimen, closer view on right).

Fig. 8—Typical failure mode for C70/40 (same specimen, closer view on right).

The mode of failure in SFRC, however, is significantly different from that of plain concrete, as seen in the typical crack patterns of Fig. 7 and 8, for normal- and high-strength concretes, respectively.

Each of the figures shows one side of a tested specimen on the left and a closer view of the cracks on the right. Generally, failure occurs with the propagation of a vertical crack band that is approximately 10 mm wide. In some cases, there is secondary tensile cracking, that is, a crack starts at Point 1 (refer to Fig. 7) and develops to a length of approximately 10 to 15 mm (shown as dashed lines in Fig. 7).

This secondary crack is later arrested and the shear crack band develops along Plane 2-2. It appears that the fibres limit the opening of the tensile cracks, leading to a shear-dominated failure in the SFRC. This justifies the use of the present test methodology to study the shear failure response of fibre concrete, even though it is not entirely suitable for the analysis of such failure in plain concrete.

### Load-displacement response

Figure 9 and 10 show the typical stress-versus-slip responses for the C30 and C70 concretes, respectively. Note that the nominal shear stress is obtained by dividing the applied load by the nominal shear-plane area of 93.8 $cm^2$.

For the plain concretes, a practically linear response can be observed up to brittle failure. The behaviour of the SFRC specimens is significantly different; the response is linear up to the first crack (indicated by a peak), followed by nonlinear behaviour. After the first peak, the load in the C30 fibre concretes tends to decrease gradually, indicating that the fibres do not affect the maximum load but cause a significant toughening effect. For higher fibre densities, as in the case of the C70 fibre concretes, there is an increase in the stress after the first peak (marked as "A" in Fig. 10), which is bigger for the higher fibre dosage, followed by a gradually decreasing post-peak response with significant residual strengths. The maximum shear stresses or strengths $\tau u$, are quantified in Table 3 for all the concretes; the values clearly reflect the significant increase in shear strength in the C70 concretes.

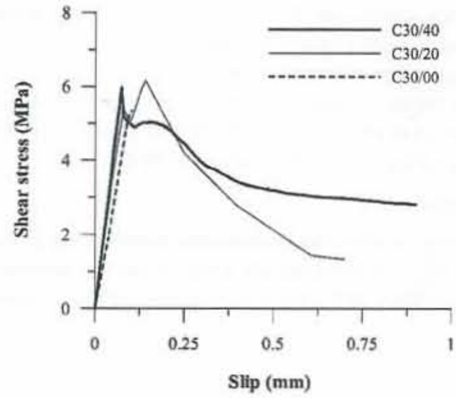


Fig. 9—Shear stress versus slip relationship for C30 concretes.

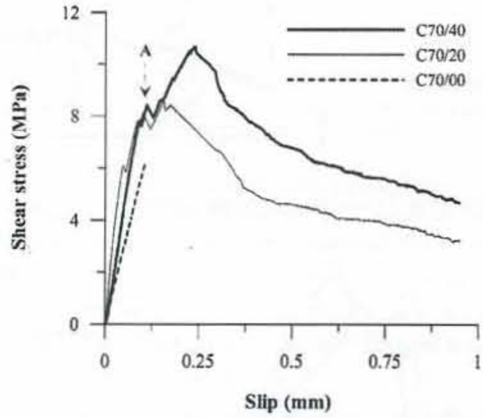


Fig. 10—Shear stress versus slip relationship for C70 concretes. (Note: "A" denotes first peak.)

It should be noted that the C70 concrete had shorter fibers with the same aspect ratio as the fibres in the C30 concrete, which results in a much higher density of fibres in the former case for the same dosage.[19] The toughening observed in the tests is a result of the pullout and dowel action of the fibers during the shear cracking. The pullout resistance tends to close the crack while the shear forces tend to open it due to the irregularity of the crack faces and aggregate interlock, as illustrated in Fig. 11. This produces a confining effect, which together with the dowel action of the fibers and friction between the crack faces, can lead to an increase in the shear strength and/or post-peak toughening, especially when the fibre density is high and there is better fibre-matrix bond. This is in accordance with the conclusions of the work of Walraven and Stroband,[20] where push-off specimens with traditional reinforcement or external restraint were studied.

The failure process can be further explained with the help of Fig. 12 (showing typical load versus slip and load versus crack width curves) and Fig. 13 (showing the corresponding curves of crack width versus slip). Until Point A (that is, the first crack), the matrix dominates the response, with negligible crack opening; beyond this point, the crack opens much further. Between first cracking and the maximum load (that is, Point B), the fibres are progressively activated and the matrix cracks completely. Thereafter, the shear fracture localizes in a dilating microcrack band, with the stresses being transferred through the fibres. There is a linear relation between the slip and crack width during this stage.

### Toughness in shear failure

Traditionally, toughness of SFRC is defined in terms of the load-displacement response of a specimen under flexural load. There are

## Shear failure of steel fibre-reinforced concrete based on push off tests

several possible measures of toughness that can be defined in terms of this response, as discussed by Gopalaratnam and Gettu.21 Most of them are based on the shape or area under the load-displacement curve until a certain prescribed limit. Such approaches have been extended herein to permit the evaluation of shear toughness using the load-slip curve obtained in the push-off test.

### Absolute toughness

First, the shear toughness is analyzed considering the absolute toughness $B^S_{s_{lim}}$, defined as the area under the stressslip curve until any prescribed slip limit $s_{lim}$ where $T^s$ is the shear stress at the slip $s$.

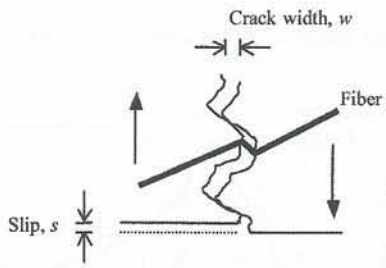


*Fig. 11–Displacement along cracked shear plane.*

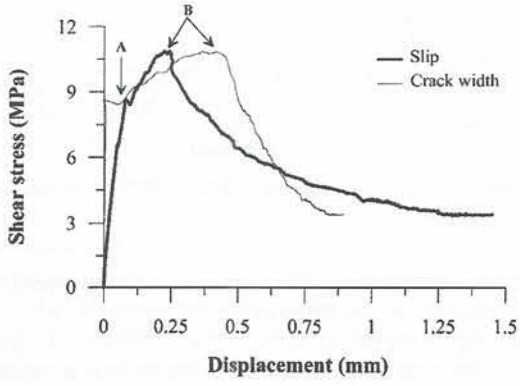


*Fig. 12–Load versus slip and crack width relationships. (Note: "A" denotes first peak and "B" denotes maximum load.)*

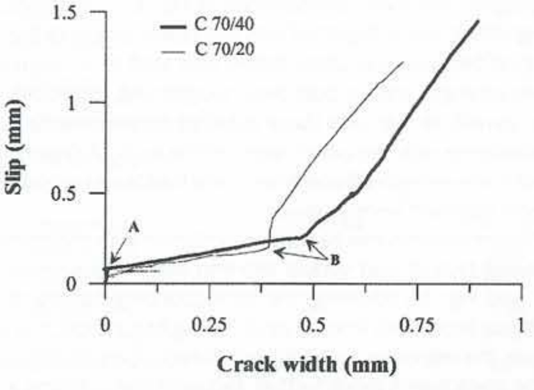


*Fig. 13–Crack width versus slip relationship. (Note: "A" denotes first peak and "B" denotes maximum load.)*

$$B^S_{s_{lim}} = \int_0^{s_{lim}} \tau^S(s)ds$$

Its evolution with an increase in slip limit can be seen in Fig. 14 and 15 for the C30 and C70 concretes, respectively. The choice of the slip limit has to be made considering the application, just as in the case of tensile toughening measures.[21]

For the C30/20 and C30/40 concretes, the absolute toughness does not exhibit a clear increase when 40 kg/m³ of fibres are used instead of 20 kg/m³, which is to be expected because the shapes of the stress-slip curves are similar. In the case of the C70 concretes, however, the trends clearly reflect the increase in toughness with an increase in fibre dosage, with larger differences at higher slip limits. For example, a 45% increase is achieved at a slip of 1 mm when the amount of fibres increases from 20 to 40 kg/m³.

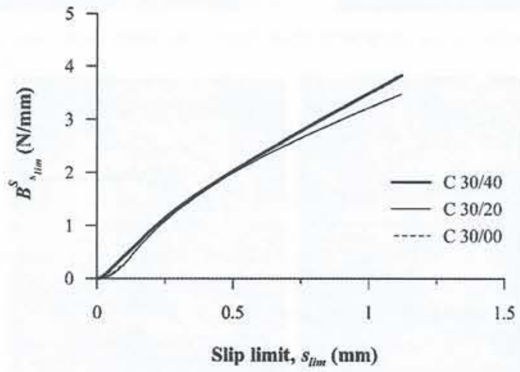


*Fig. 14–Evolution of absolute toughness with slip limit (for C30 concretes).*

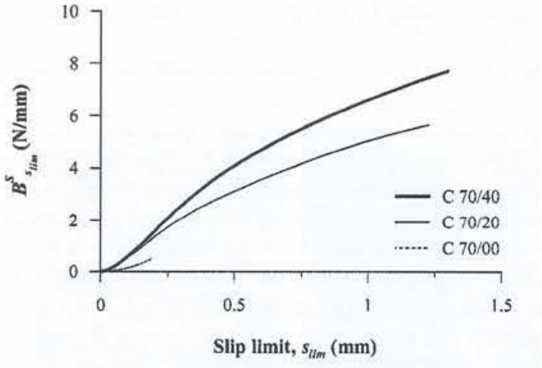


*Fig. 15–Evolution of absolute toughness with slip limit (for C70 concretes).*

### Table 4—Eqivalent shear strength results

| Concrete | Eqivalent shear strength results $f^S_{s_{lim}}$, MPa | | |
|---|---|---|---|
| | $f^S_{0.25}$ | $f^S_{0.50}$ | $f^S_{1.00}$ |
| 30/20 | 4.7 | 4.1 | 3.7 |
| 30/40 | 4.5 | 3.9 | 3.8 |
| 70/20 | 6.4 | 5.9 | 4.6 |
| 70/40 | 7.3 | 7.1 | 6.6 |

### Equivalent shear strength

As in the case of the equivalent flexural strength, which has already been introduced in design recommendations for SFRC,[22] the equivalent shear strength can be obtained as

$$f^S_{s_{lim}} = \frac{B^S_{s_{lim}}}{s_{lim}}$$

Average values of equivalent shear strength up to slip limits $s_{lim}$ = 0.25, 0.5, and 1.0 mm are presented in Table 4, where the values are averages from three specimens. As in the absolute toughness, the incorporation of 40 kg/m³ of fibres in the C70 concrete leads to a 45% increase of $f^{S}$ 1.00 with respect to the concrete containing 20 kg/m$^3$ of fibres whereas the values are similar for the C30 concretes.

### Residual shear strength

The residual strength can be considered to be a direct measure of the effective stress that can be transferred across an open crack. Table 5 shows the results of the residual strength at the same slip limits considered for the equivalent shear strength.

Table 5—Residual shear strength results

| Concrete | Residual strength $\tau^{s_{lim}}_{res}$, Mpa | | |
|---|---|---|---|
| | $\tau^{0.25}_{res}$ | $\tau^{0.50}_{res}$ | $\tau^{1.00}_{res}$ |
| 30/20 | 4.7 | 2.7 | 2.7 |
| 30/40 | 4.1 | 3.1 | 3.2 |
| 70/20 | 6.9 | 4.2 | 2.6 |
| 70/40 | 8.7 | 5.8 | 4.3 |

The trends are the same as those observed earlier, though the residual strength for the C30 concrete seems to increase slightly with an increase in fibre dosage at larger slips. Nevertheless, the increases observed in the C70 concrete are much more significant.

## CONCLUSIONS

Tests of notched specimens in the push-off configuration demonstrate the energy dissipation capacity of steel fibre-reinforced concrete in the post-cracking regime. The incorporation of fibres in concrete subjected to shear leads to a better mechanical integrity during failure. The pullout resistance and dowel action of the fibres can lead to considerable residual load-carrying capacity in shear dominated failure.

Significant improvements in the ductility of concrete during shear failure and some increase in the shear strength are achieved through the incorporation of steel fibres in both normal- and high-strength concretes.

The knowledge of the shear stress that can be transferred across an open crack is of great importance for fracture mechanics-based design approaches, where residual and/or equivalent shear strengths could be integrated along the sections of the structural element subjected to shear to calculate its shear load-carrying capacity. Studies on the enhancement of the shear cracking resistance of the web-flange interface in pre-stressed concrete I-beams have been carried out with promising results at the Universitat Politècnica de Catalunya, with promising results.[23] On the other hand, because the push-off test is simple, it can be used to assess the shear strength of SFRC for its incorporation in code-type structural design procedures. Nevertheless, because the fibres tend to have a preferential orientation,[17] due to the vibration during the compaction of the concrete or the placing procedure, the laboratory tests should be performed such that the failure plane represents the fibre distribution in the structural element.

## ACKNOWLEDGMENTS

The present study was partially supported by the Spanish CICYT grants MAT96-0967 and MAT2003-5530 to the Universitat Politècnica de Catalunya (UPC), Barcelona, Spain. The materials used in this work were donated by Bekaert, Cementos Molins, and Grace. The authors especially thank R. de Fátima Zalochi for her contribution in the development of the tests and analysis of the results, and E. Terré and H. Saldivar for the preliminary studies. The tests were performed at the Structural Technology Laboratory at UPC.

## NOTATION

$B^S_{0.25}$ = absolute thoughness until slip limit of 0.25 mm
$B^S_{0.50}$ = absolute thoughness until slip limit of 0.50 mm
$B^S_{1.00}$ = absolute thoughness until slip limit of 1.00 mm
$B^S_{slim}$ = absolute thoughness until slip limit of $s_{lim}$
$E$ = modulus of elascity
$f_c$ = mean value of comprehensive strength
$f^S_{0.25}$ = equivalent flexural strength up to slip limit of 0.25 mm
$f^S_{0.50}$ = equivalent flexural strength up to slip limit of 0.50 mm
$f^S_{1.00}$ = equivalent flexural strength up to slip limit of 01.00 mm
$f^S_{slim}$ = equivalent flexural strength up to slip limit of $s_{lim}$
$\tau^{res}_{0.25}$ = residual strength at slip of 0.25 mm
$\tau^{res}_{0.50}$ = residual strength at slip of 0.50 mm
$\tau^{res}_{1.00}$ = residual strength at slip of 1.00 mm
$\tau^{res}_{slim}$ = residual strength at slip of $s_{lim}$

## REFERENCES

1. Vandewalle, L., and Dupont, D., eds., "Test and Design Methods for Steel Fiber Reinforced Concrete," *Report of Brite Euram Project* BRPRCT98-0813, 2003. (CD-ROM)

2. Barr, B., "The Fracture Characteristics of FRC Materials in Shear," *Fiber Reinforced Concrete: Properties and Applications*, SP-105, S. P. Shah and G. B. Batson, eds., American Concrete Institute, Farmington Hills, Mich., 1987, pp. 27-53.

3. Barr, B.; Gettu, R.; Al-Oraimi, S. K. A.; and Bryars, L. S., "Toughness Measurement—The Need to Think Again," *Cement and Concrete Composites*, V. 18, 1996, pp. 281-297.

4. JSCE-SF6, "Method of Test for Shear Strength of Steel Fiber Reinforced Concrete (SFRC)," Japan Society of Civil Engineers, Tokyo, 1990, pp. 67-69.

5. Mirsayah, A. A., and Banthia, N., "Shear Strength of Steel Fiber-Reinforced Concrete," *ACI Materials Journal*, V. 99, No. 5, Sept.-Oct. 2002, pp. 473-479.

6. Liu, K.; Barr, B. I. G.; and Watkins, J., "Mode II Fracture of Fiber Reinforced Concrete Materials," *International Journal of Cement Composites and Lightweight Concrete*, V. 7, No. 2, 1985, pp. 93-101.

7. Swamy, R.; Jones, R.; and Chiam, T., "Shear Transfer in Steel Fiber Reinforced Concrete," *Fiber Reinforced Concrete: Properties and Applications*, SP-105, S. P. Shah and G. B. Batson, eds., American Concrete Institute, Farmington Hills, Mich., 1987, pp. 565-593.

8. Allos, A. E., "Shear Transfer in Fibre Reinforced Concrete," *Fiber Reinforced Cement and Concretes: Recent Developments*, R. N. Swamy and B. Barr, eds., Elsevier Applied Science, London, 1989, pp. 146-156.

9. Benaiche, F., and Barr, B., "Fracture Characteristics of High Strength Concrete and FRC Materials," *Fiber Reinforced Cement and Concretes: Recent Developments*, R. N. Swamy and B. Barr, eds., Elsevier Applied Science, London, 1989, pp. 411-419.

10. Tan, K. H., and Mansur, M. A., "Shear Transfer in Reinforced Fiber Concrete," *Journal of Materials in Civil Engineering*, V. 2, No. 4, 1990, pp. 202-214.

11. Balaguru, P., and Dipsia, M. G., "Properties of Fiber Reinforced High-Strength Semilightweight Concrete," *ACI Materials Journal*, V. 90, No. 5, Sept.-Oct. 1993, pp. 399-405.

12. Valle, M., and Büyüköztürk, O., "Behavior of Fiber Reinforced High-Strength Concrete under Direct Shear," *ACI Materials Journal*, V. 90, No. 2, Mar.-Apr. 1993, pp. 122-133.

13. Khaloo, A. R., and Kim, N., "Influence of Concrete and Fiber Characteristics on Behavior of Steel Fiber Reinforced Concrete under Direct Shear," *ACI Materials Journal*, V. 94, No. 6, Nov.-Dec. 1997, pp. 592-601.

14. del Giorgio, F., and Trintinaglia, C., "Shear Fracture of Plain and Fiber Reinforced Concrete: Study with a Non-Local Damage Model," Laureate Thesis, Politecnico di Milano, Milan, Italy, 2000. (in Italian)

15. Vandewalle, L., "Influence of Tensile Strength of Steel Fibre on Toughness of High Strength Concrete," *Proceedings of Third International Workshop on High-Performance Cement Composites* (Mainz, Germany), H. W. Reinhardt and A. E. Naaman, eds., RILEM Publications, Bagneux, France, 1999, pp. 331-337.

16. RILEM TC 162-TDF Recommendations, "Test and Design Methods for Steel Fiber Reinforced Concrete: Bending Test," *Materials and Structures*, V. 33, 2000, pp. 3-5.

17. Gettu, R.; Gardner, D. R.; Saldívar, H.; and Barragán, B. E., "Study of the Distribution of Orientation of Fibers in SFRC Specimens," *Materials and Structures*, V. 38, 2005, pp. 31-37.

18. van Mier, J. G. M., *Fracture Processes of Concrete*, CRC Press, Boca Raton, Fla., 1997, 460 pp.

19. Romualdi, J. P., and Mandel, J. A., "Tensile Strength of Concrete Affected by Uniformly Distributed and Closely Spaced Short Lengths of Wire Reinforcement," ACI JOURNAL, *Proceedings* V. 61, 1964, pp. 657-672.

20. Walraven, J., and Stroband, J., "Shear Friction in High-Strength Concrete," *High-Performance Concrete*, Proceedings of the ACI International Conference, SP-149, V. M. Malhotra, ed., Farmington Hills, Mich., 1994, pp. 311-330.

21. Gopalaratnam, V. S., and Gettu, R., "On the Characterization of Flexural Toughness in Fiber Reinforced Concretes," *Cement and Concrete Composites*, V. 17, 1995, pp. 239-254.

22. RILEM TC 162-TDF Recommendations, "Test and Design Methods for Steel Fiber Reinforced Concrete: σ-ε Design Method," *Materials and Structures*, V. 33, 2000, pp. 75-81.

23. Barragán, B. E., "Failure and Toughness of Steel Fiber Reinforced Concrete under Tension and Shear," doctoral thesis, Universitat Politècnica de Catalunya, Barcelona, Spain, 2002, http://www.tdx.cesca.es/TDCat 1205102-083658/.